Inelastic Neutron-Scattering Measurements of a Three-Dimensional Spin Resonance in the FeAs-Based $BaFe_{1.9}Ni_{0.1}As_2$ Superconductor

Songxue Chi,[1] Astrid Schneidewind,[2] Jun Zhao,[1] Leland W. Harriger,[1] Linjun Li,[3] Yongkang Luo,[3] Guanghan Cao,[3] Zhu'an Xu,[3] Micheal Loewenhaupt,[2] Jiangping Hu,[4] and Pengcheng Dai[1,5,*]

[1]*Department of Physics and Astronomy, The University of Tennessee, Knoxville, Tennessee 37996-1200, USA*
[2]*Technische Universität Dresden, Institut für Festkörperphysik, 01062 Dresden, Germany*
[3]*Department of Physics, Zhejiang University, Hangzhou 310027, China*
[4]*Department of Physics, Purdue University, West Lafayette, Indiana 47907, USA*
[5]*Neutron Scattering Science Division, Oak Ridge National Laboratory, Oak Ridge, Tennessee 37831-6393, USA*

(Received 6 December 2008; published 12 March 2009)

We use inelastic neutron scattering to study magnetic excitations of the FeAs-based superconductor $BaFe_{1.9}Ni_{0.1}As_2$ above and below its T_c (=20 K). In addition to gradually open a spin gap at the in-plane antiferromagnetic ordering wave vector (1, 0, 0), the effect of superconductivity is to form a three-dimensional resonance with clear dispersion along the c axis. The intensity of the resonance develops like a superconducting order parameter, and the mode occurs at distinctively different energies at (1, 0, 0) and (1, 0, 1). If the resonance energy is associated with the superconducting gap energy Δ, then Δ is dependent on the wave vector transfers along the c axis. These results suggest that one must be careful in interpreting the superconducting gap energies obtained by surface sensitive probes such as scanning tunneling microscopy and angle resolved photoemission.

DOI: 10.1103/PhysRevLett.102.107006 PACS numbers: 74.25.Ha, 74.70.−b, 78.70.Nx

Understanding the interplay between spin fluctuations and superconductivity in high-transition-temperature (high-T_c) superconductors is important because spin fluctuations may mediate electron pairing for superconductivity. In the case of high-T_c copper oxides, it is now well documented that the spin fluctuation spectrum is dominated by a collective excitation known as the resonance mode centered at the antiferromagnetic (AF) ordering wave vector $Q = (1/2, 1/2)$ [1–5]. A similar mode has also been observed in heavy fermion superconductors UPd_2Al_3 [6] and $CeCoIn_5$ [7]. Although the intensity of the mode behaves like an order parameter below T_c, the energy of the mode is dispersionless for wave vector transfers (Q) along the c axis and directly tracks T_c [2–5], thus suggesting that the mode is an intrinsic property of the two-dimensional (2D) CuO_2 planes and intimately associated with superconductivity. For FeAs-based superconductors [8–11], the presence of static AF ordering in their parent compounds [with spin structure of Fig. 1(a)] [12–16] and the remarkably similar doping dependent phase diagram to that of the high-T_c copper oxides [13] suggest that AF spin fluctuations may also play an important role in the superconductivity of these materials. Indeed, recent neutron-scattering measurements on spin fluctuations of powder samples of superconducting $Ba_{0.6}K_{0.4}Fe_2As_2$ ($T_c = 38$ K) [17] and crystalline electric field excitations of Ce in $CeFeAsO_{0.84}F_{0.16}$ ($T_c = 41$ K) [18] found clear evidence for resonant-like magnetic intensity gain below T_c at $\hbar\omega \sim$ 14 and 18.7 meV, respectively. However, the Ce crystalline electric field measurements give no information on the Q dependence of the scattering [18]. Although the resonant-like scattering in $Ba_{0.6}K_{0.4}Fe_2As_2$ occurs near the AF ordering wave vector, the powder nature of the experiment impedes to distinguish whether the resonant scattering is centered at the three-dimensional (3D) AF wave vector $Q = (1, 0, 1)$ of its parent compound [14–16] or simply at a 2D AF in-plane wave vector $Q = (1, 0, 0)$ [17].

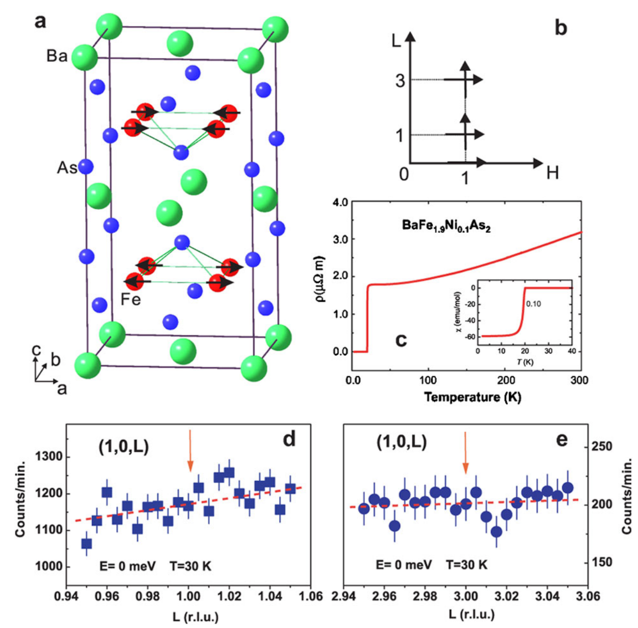

FIG. 1 (color online). (a) Schematic diagram of the Fe spin ordering in the $BaFe_2As_2$ and we use the same unit cell for $BaFe_{1.9}Ni_{0.1}As_2$ for easy comparison. (b) Reciprocal space probed in our experiment. (c) Resistivity and magnetic susceptibility measurements of T_c. (d,e) Elastic neutron-scattering L scans through (1, 0, 1) and (1, 0, 3) magnetic Bragg peaks at 30 K, showing no evidence of static long-range AF order [15,16].

In this Letter, we report the results of inelastic neutron-scattering studies of spin fluctuations in single crystals of superconducting $BaFe_{1.9}Ni_{0.1}As_2$ [$T_c = 20$ K, Fig. 1(c)] [11]. We show that the effect of superconductivity is to gradually open a low-energy spin gap and also to induce a resonance at energies above the spin gap energy. Although the intensity of the resonance develops below T_c similar to that of the resonance in high-T_c copper oxides, the mode actually has a dispersion along the c axis, and occurs at distinctively different energies at $Q = (1, 0, 1)$ and $(1, 0, 0)$ in contrast with the cuprates. If the resonance energy in FeAs superconductors is associated with the superconducting gap energy Δ, then Δ should be 3D in nature and depend sensitively on the Q values along the c axis.

We grew high quality $BaFe_{1.9}Ni_{0.1}As_2$ single crystals (each with mosaicity $<0.5°$) using the flux method [11]. Figure 1(c) shows resistivity and magnetic susceptibility data of a typical crystal showing an onset T_c of 20.2 K with a transition width less than 1 K. We coaligned 21 single crystals on a flat Al plate to obtain a total mass of about 0.6 grams. The in-plane mosaic of the aligned crystal assembly is about 1.3° and the out-of-plane mosaic is less than 4.3° full width at half maximum. Our neutron-scattering experiments were performed on the PANDA cold triple-axis spectrometer at the Forschungs-neutronenquelle Heinz Maier-Leibnitz (FRM II), TU München, Germany. We used pyrolytic graphite (0,0,2) as monochromator and analyzer without any collimator. We defined the wave vector Q at (q_x, q_y, q_z) as $(H, K, L) = (q_x a/2\pi, q_y b/2\pi, q_z c/2\pi)$ reciprocal lattice units (rlu) using the orthorhombic magnetic unit cell [14–16] of the parent undoped compound (space group $Fmmm$, $a = 5.564$, $b = 5.564$, and $c = 12.77$ Å). We choose this reciprocal space notation (although the actual crystal structure is tetragonal) for easy comparison with previous spin-wave and elastic measurements on the parent compound, where magnetic Bragg peaks and low-energy spin waves are expected to occur around (1, 0, 1) and (1, 0, 3) rlu positions [see Fig. 1(b)] [19–21]. For the experiment, the $BaFe_{1.9}Ni_{0.1}As_2$ crystal assembly was mounted in the [H, 0, L] zone inside a closed cycle refrigerator. The final neutron wave vector was fixed at either $k_f = 1.55$ Å^{-1} with a cold Be filter or at $k_f = 2.662$ Å^{-1} with a pyrolytic graphite filter in front of the analyzer.

We first searched for possible static AF order in our samples. For undoped $BaFe_2As_2$, magnetic Bragg peaks are expected at the (1, 0, 1) and (1, 0, 3) positions for the spin structure of Fig. 1(a) [14]. In addition, the low-temperature spin waves have an anisotropy gap of about 9.8 meV [21]. Our elastic Q scans through these expected AF Bragg peak positions are featureless [Figs. 1(d) and 1(e)], confirming the absence of static long-range order above 30 K. Figure 2 summarizes constant-energy scans at 3 K (well below T_c) and at 30 K (above T_c) at $\hbar\omega = 2, 6$, and 8.5 meV carried out with $k_f = 1.55$ Å^{-1}. Although these probed energies are well below the 9.8 meV spin gap energy in the parent compound [21], we observe at 30 K clear peaks centered at the in-plane AF wave vector (1, 0, 0) for $\hbar\omega = 2$ and 6 meV, and half of a peak at $\hbar\omega = 8.5$ meV due to kinematic constraints [Figs. 2(a)–2(c)]. Fourier transforms of the Gaussian peaks in Figs. 2(a) and 2(b) gave the minimum dynamic spin correlation lengths of $\xi \approx 16 \pm 4$ and 21 ± 4 Å for $\hbar\omega = 2$ and 6 meV, respectively. The spin-spin correlations extend only to several chemical unit cells and are much smaller than the $\xi \approx 80 \pm 10$ Å at $\hbar\omega = 1.5$ meV obtained for electron-doped cuprate superconductor $Pr_{0.88}LaCe_{0.12}CuO_4$ [4]. On cooling from 30 to 3 K, the Gaussian peak at $\hbar\omega = 2$ meV vanishes and suggests the opening of a spin gap [Figs. 2(a)]. In contrast, the Gaussian peaks at $\hbar\omega = 6$ meV hardly change across T_c [Fig. 2(b)], whereas the scattering at (1, 0, 0) for $\hbar\omega = 8.5$ meV actually increases below T_c [Fig. 2(c)]. These results are similar to those for electron-doped $Nd_{1.85}Ce_{0.15}CuO_4$ [5], and immediately suggest that the opening of a low-energy spin gap below T_c is compensated by intensity gain above the gap energy. The low-temperature $(1, 0, L)$ scan at $\hbar\omega = 8.5$ meV shows two broad peaks centered at $(1, 0, -1)$ and (1, 0, 1) corresponding to the 3D AF ordering wave vector [14–16].

To determine the size of the superconducting spin gap and confirm the intensity gain at $\hbar\omega = 8.5$ meV below T_c, we carried out energy scans at $Q = (1, 0, 0)$ below and

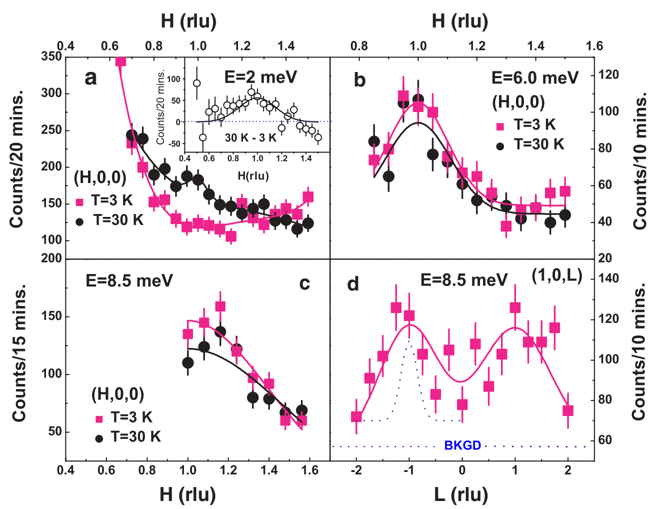

FIG. 2 (color online). Constant-energy scans around the (1, 0, 0) and (1, 0, 1) positions for $\hbar\omega = 2$, 6, and 8.5 meV obtained with $k_f = 1.55$ Å^{-1}. (a–c) Q scan along the $[H, 0, 0]$ direction for $\hbar\omega = 2$, 6, and 8 meV at 30 and 3 K. The inset in (a) shows the temperature difference plot and a Gaussian fit to the data. The missing low-Q data for scans in (b) and (c) are due to kinematic constraint. (d) Q scan along the $[1, 0, L]$ direction for $\hbar\omega = 8.5$ meV at 3 K. Note two clear peaks centered at (1, 0, -1) and (1, 0, 1), respectively. The dashed-line peak is the low-temperature spin waves of $BaFe_2As_2$ at $\hbar\omega = 10$ meV from Fig. 2f in [21].

above T_c [Fig. 3(a)]. While the background scattering collected at $Q = (1.3, 0, 0)$ (not shown) changes only negligibly between 30 and 3 K, intensity at $Q = (1, 0, 0)$ is suppressed for $\hbar\omega \le 4$ meV and enhanced for $\hbar\omega \ge 6$ meV with the highest intensity at $\hbar\omega = 9$ meV. In Fig. 3(b), we plot the difference (3 K minus 30 K) of the scattering at $Q = (1, 0, 0)$, again confirming the opening of a spin gap for $\hbar\omega \le 4$ meV and enhanced magnetic scattering for $\hbar\omega \ge 6$ meV in the superconducting state. Figure 3(c) shows the temperature dependence of the scattering at $Q = (1, 0, 0)$ and $\hbar\omega = 2$ meV. The solid line shows the expected magnetic intensity change due to the Bose population factor; it is clear that the intensity reduction below 15 K is not due to simple Bose statistics. The results suggest that the spin gap in $BaFe_{1.9}Ni_{0.1}As_2$ opens gradually with decreasing temperature until it reaches about 4 meV at 3 K (confirmed by recent measurements), remarkably similar to the spin gap behavior of electron-doped $Nd_{1.85}Ce_{0.15}CuO_4$ [5,22].

Although the results displayed in Figs. 1–3 using $k_f = 1.55$ Å^{-1} are suggestive of a resonance below T_c, kinematic constraints did not allow us to carry out measurements for energies above $\hbar\omega = 9$ meV at $Q = (1, 0, 0)$. To determine the energy location of the possible mode, we collected additional data with $k_f = 2.662$ Å^{-1}. Figure 4(a) shows the energy scan raw data at $Q = (1, 0, 0)$ below and above T_c. Inspection of the data reveals that the low-temperature scattering enhances dramatically around $\hbar\omega = 9.0$ meV compared to the normal state scattering. Since Bose population factor does not contribute much to magnetic scattering intensity for $\hbar\omega \ge 5$ meV between 3 and 30 K, the (low minus high) temperature difference scattering represents the net magnetic intensity gain at low temperature. Subtracting the 30 K data from the 3 K data reveals a clear localized mode near 9.0 meV [Fig. 4(b)]. Gaussian fit to the data gives a peak position $\hbar\omega = 9.1 \pm 0.4$ meV, a peak width 3.3 ± 0.9 meV, and an integrated area 346 ± 82 per 20 minutes [Fig. 4(b)].

Since spin excitations at $\hbar\omega = 8.5$ meV peak at $(1, 0, -1)/(1, 0, 1)$ and have clear c axis modulation

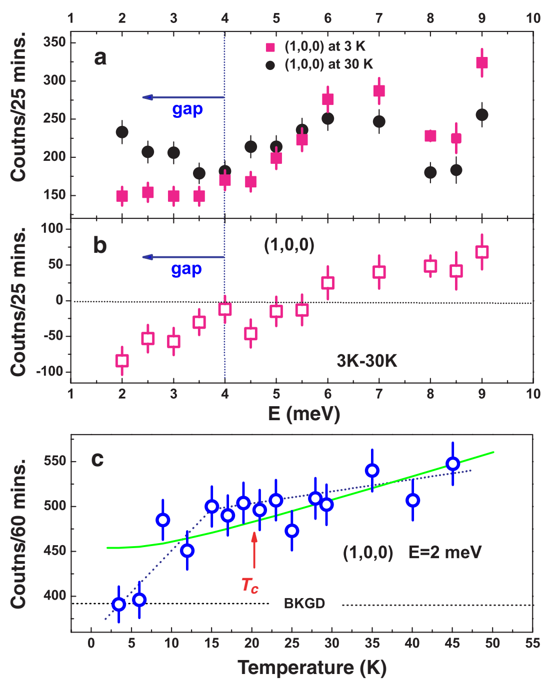

FIG. 3 (color online). (a) Energy scans at $Q = (1, 0, 0)$ from 2 to 9 meV at 30 and 3 K with $k_f = 1.55$ Å^{-1}. The broad peak in energy near 6 meV was also seen in the background scattering collected at the (1.3, 0, 0) position (not shown) and were not intrinsic properties of the material. (b) Intensity difference between the 3 and 30 K data at $Q = (1, 0, 0)$. The negative scattering below 4 meV indicates the opening of a spin gap, while positive scattering above 6 meV suggests a magnetic intensity gain below T_c. (c) Temperature dependence of the scattering obtained at $Q = (1, 0, 0)$ and $\hbar\omega = 2$ meV with the vertical arrow indicating T_c. The solid line shows the expected T-dependent scattering due to the Bose population factor.

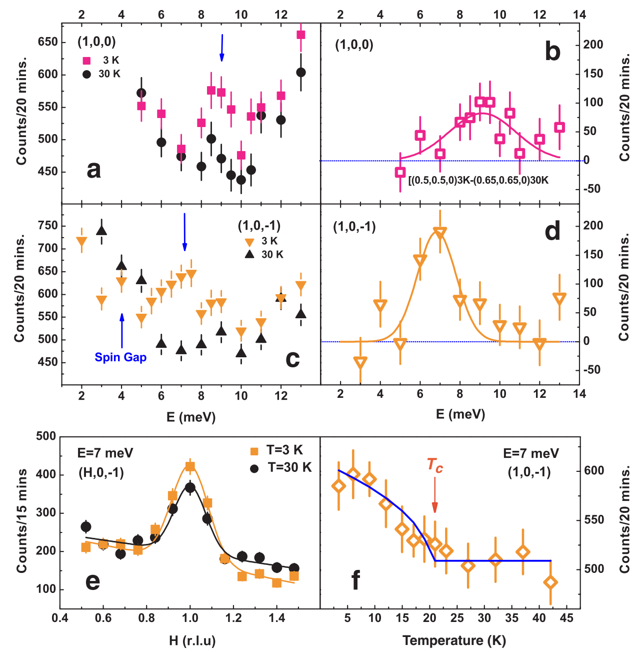

FIG. 4 (color online). (a) Energy scans at $Q = (1, 0, 0)$ from 5 to 13 meV at 30 and 3 K with $k_f = 2.662$ Å^{-1}. The background scattering at $Q = (1.3, 0, -1)$ is weakly T dependent between 30 and 3 K. (b) The temperature difference scattering between 3 and 30 K shows a clear resonant peak at $\hbar\omega = 9.1 \pm 0.4$ meV. (c) Energy scans at $Q = (1, 0, -1)$ from 2 to 13 meV at 30 and 3 K. (d) The temperature difference plot confirms that the mode has now moved to 7.0 ± 0.5 meV. (e) Wave vector dependence of the scattering at 30 and 3 K for $\hbar\omega = 7$ meV, confirming that the resonance intensity gain occurs at $Q = (1, 0, -1)$. (f) Temperature dependence of the scattering at $Q = (1, 0, -1)$ and $\hbar\omega = 7$ meV shows a clear order-parameter-like increase below T_c. The solid line is the best fit to the data using $I = I_0 + k(1 - (T/T_c))^\beta$ yielding $\beta = 0.5$ and $T_c = 20$ K. The intensity differences in (c) and (f) are within 2σ.

[Fig. 2(d)], we carried out additional measurements to search for resonance at the 3D AF ordering wave vector $Q = (1, 0, -1)$ below and above T_c. The outcome in Fig. 4(c) shows a large magnetic intensity gain below T_c at $\hbar\omega = 7$ meV, clearly different from the 9.1 meV resonance at $Q = (1, 0, 0)$. A Gaussian fit to the temperature difference plot in Fig. 4(d) gives a peak position $\hbar\omega = 7.0 \pm 0.5$ meV, a peak width 1.9 ± 0.7 meV, and an integrated area of 464 ± 145 per 20 minutes. To further confirm that the intensity gain at $\hbar\omega = 7$ meV is indeed the resonance occurring at $Q = (1, 0, -1)$, we carried constant-energy scans around (1, 0, −1) and the outcome clearly shows that the intensity gain below T_c arises from scattering at the 3D AF ordering position [Fig. 4(e)]. Finally, in Fig. 4(f) we plot the temperature dependence of the scattering at (1, 0, −1) and $\hbar\omega = 7$ meV. The scattering increases dramatically below the onset of T_c and is remarkably similar to that of the resonance in high-T_c copper oxides [1–5].

If the resonance is a measure of electron pairing correlations in high-T_c superconductors [23], the observed 3D resonance dispersion in $BaFe_{1.9}Ni_{0.1}As_2$ would suggest a variation of the superconducting gap Δ along the c axis, similar to those in UPd_2Al_3 [24]. This is quite different from the high-T_c copper oxides, where Δ is strictly 2D and independent of the c axis modulations. For FeAs-based superconductors, the resonance may arise from quasiparticle transitions across the sign-revised s-wave electron (Δ_0^e) and hole (Δ_0^h) superconducting gaps in pure two-dimensional models [25–30]. By considering the AF coupling between layers, the gap functions can be naturally modified to $\Delta_e(k_z) = \Delta_e^0 + \delta\cos(k_z)$ and $\Delta_h(k_z) = \Delta_h^0 + \delta\cos(k_z)$. For a sign-revised s pairing symmetry, $\Delta_0^e \sim -\Delta_0^h \sim -\Delta_0$. Therefore, the dispersion of the resonance along the c axis is roughly determined by [26]

$$\hbar\omega(q_z) \sim \min[\langle|\Delta_e(k_z)| + |\Delta_h(k_z + q_z)|\rangle, k_z] \sim 2\Delta_0 - 2\delta\left|\sin\left(\frac{q_z}{2}\right)\right|. \quad (1)$$

Based on this interpretation, our experimental results suggest $\delta/\Delta_0 = [\omega(1, 0, 0) - \omega(1, 0, -1)]/\omega(1, 0, 0) = 0.26 \pm 0.07$. If spin fluctuations are responsible for electron pairing and superconductivity, the values Δ_0 and δ are expected to be proportional to the intraplane and interplane AF couplings, $J_\parallel$ and $J_\perp$, respectively, which naturally suggests $\delta/\Delta_0 \sim J_\perp/J_\parallel$. The ratio δ/Δ_0 determined by our resonance dispersion is a reasonable agreement with the ratio of the AF exchange couplings measured by neutron-scattering experiments in the parent compounds [19–21]. These results suggest that spin fluctuations are also important for superconductivity in FeAs-based superconductors.

This work is supported by the U.S. NSF No. DMR-0756568, U.S. DOE BES No. DE-FG02-05ER46202, and in part by the U.S. DOE, Division of Scientific User Facilities. The work at Zhejiang University is supported by the NSF of China. We further acknowledge support from DFG within Sonderforschungsbereich 463 and from the PANDA project of TU Dresden and FRM II.

Note added.—After finishing the present work, we became aware of a preprint where the resonance at $\hbar\omega = 9.5$ meV was reported near $Q = (1, 0, 0)$ in superconducting $BaFe_{1.84}Co_{0.16}As_2$ ($T_c = 22$ K) [31].

*daip@ornl.gov

[1] J. Rossat-Mignod *et al.*, Physica C (Amsterdam) **185**, 86 (1991).
[2] H. A. Mook *et al.*, Phys. Rev. Lett. **70**, 3490 (1993).
[3] C. Stock *et al.*, Phys. Rev. B **69**, 014502 (2004).
[4] S. D. Wilson *et al.*, Nature (London) **442**, 59 (2006).
[5] J. Zhao *et al.*, Phys. Rev. Lett. **99**, 017001 (2007).
[6] N. Metoki *et al.*, Phys. Rev. Lett. **80**, 5417 (1998).
[7] C. Stock *et al.*, Phys. Rev. Lett. **100**, 087001 (2008).
[8] Y. Kamihara *et al.*, J. Am. Chem. Soc. **130**, 3296 (2008).
[9] M. Rotter *et al.*, Phys. Rev. Lett. **101**, 107006 (2008).
[10] A. S. Sefat *et al.*, Phys. Rev. Lett. **101**, 117004 (2008).
[11] L. J. Li *et al.*, New J. Phys. **11**, 025008 (2009).
[12] C. de la Cruz *et al.*, Nature (London) **453**, 899 (2008).
[13] J. Zhao *et al.*, Nature Mater. **7**, 953 (2008).
[14] Q. Huang *et al.*, Phys. Rev. Lett. **101**, 257003 (2008).
[15] J. Zhao *et al.*, Phys. Rev. B **78**, 140504(R) (2008).
[16] A. I. Goldman *et al.*, Phys. Rev. B **78**, 100506(R) (2008).
[17] A. D. Christianson *et al.*, Nature (London) **456**, 930 (2008).
[18] Songxue Chi *et al.*, Phys. Rev. Lett. **101**, 217002 (2008).
[19] J. Zhao *et al.*, Phys. Rev. Lett. **101**, 167203 (2008).
[20] R. J. McQueeney *et al.*, Phys. Rev. Lett. **101**, 227205 (2008).
[21] K. Matan *et al.*, Phys. Rev. B **79**, 054526 (2009).
[22] K. Yamada *et al.*, Phys. Rev. Lett. **90**, 137004 (2003).
[23] Pengcheng Dai *et al.*, Nature (London) **406**, 965 (2000).
[24] N. Bernhoeft, Eur. Phys. J. B **13**, 685 (2000).
[25] I. I. Mazin *et al.*, Phys. Rev. Lett. **101**, 057003 (2008).
[26] T. A. Maier and D. J. Scalapino, Phys. Rev. B **78**, 020514 (R) (2008).
[27] M. M. Korshunov and I. Eremin, Phys. Rev. B **78**, 140509 (R) (2008).
[28] A. V. Chubukov, D. V. Efremov, and I. Eremin, Phys. Rev. B **78**, 134512 (2008).
[29] K. Seo *et al.*, Phys. Rev. Lett. **101**, 206404 (2008).
[30] F. Wang *et al.*, Phys. Rev. Lett. **102**, 047005 (2009).
[31] M. D. Lumsden *et al.*, arXiv:0811.4755v1 [Phys. Rev. Lett. (to be published)].